Babylonian Journal of Mechanical Engineering
Vol.2025, **pp**. 51–67
DOI: https://doi.org/10.58496/BJME/2025/004; ISSN: 3006-5410
https://mesopotamian.press/journals/index.php/BJME

Research Article

Data-Driven Melt Pool Monitoring and Defect Prediction in LPBF of Ti-6Al-4V Alloy

Marshima Mohd Rosli [1, *], Ali Rachini[2], Musaria Karim Mahmood[3]

[1] *Informatics and Mathematics,v College of Computing, Universiti Teknologi MARA, Shah Alam, Malaysia.*
[2] *Faculty of Arts and Sciences Holy Spirit, University of Kaslik (USEK), Jounieh, Lebanon.*
[3] *Energy Systems Engineering Department, Ankara Yildirim Beyazit University, Ankara, Turkey*

ARTICLE INFO

Article History
Received 19 Jan 2025
Revised: 12 Feb 2025
Accepted 15 Mar 2025
Published 10 Apr 2025

Keywords
Polymer Nanocomposites
Mechanical Properties
Tensile Testing
Toughness Optimization

ABSTRACT

Real-time process monitoring is essential for achieving consistent part quality in Laser Powder Bed Fusion (LPBF), yet robust and practical defect prediction frameworks remain underdeveloped. This study presents a machine learning-based approach for predicting unstable melt pool conditions, leveraging an open dataset of melt pool variability measurements from Ti-6Al-4V builds on an EOS M290 system. The framework utilizes fundamental process parameters—laser velocity, power, scan orientation, and track location—combined with statistical melt pool geometry features to train a Random Forest classifier. The model achieved an accuracy of 99.79% in distinguishing between stable and unstable melt pool states, with balanced sensitivity and specificity. Analysis of defect trends across the process parameter space revealed that higher scan velocities and certain orientations significantly increase defect likelihood. The results confirm that interpretable, computationally efficient machine learning models can provide robust real-time defect prediction using features already accessible on commercial LPBF platforms. The framework offers a scalable and industry-relevant pathway toward enhanced quality assurance in metal additive manufacturing, supporting the advancement of intelligent, closed-loop LPBF process control.

1. INTRODUCTION

1.1 Importance of LPBF in Modern Manufacturing

Laser Powder Bed Fusion (LPBF) is one of the most advanced metal additive manufacturing (AM) techniques in modern industry [1]. It allows for the creation of geometrically complex parts with high material efficiency and minimal tooling requirements. LPBF has been increasingly adopted in sectors such as aerospace, biomedical implants, and automotive components due to its ability to fabricate parts from high-performance alloys like Ti-6Al-4V [2], [3]. The flexibility of LPBF enables designers to produce lightweight structures, lattice materials, and components with internal features that are difficult or impossible to achieve with traditional manufacturing methods [4].

1.2 Problems: Defects (Porosity, Lack of Fusion) → Impact Product Quality

Despite its advantages, LPBF is prone to various process-induced defects that can compromise part integrity. Among the most critical defects are porosity, lack of fusion, keyholing, and geometric inaccuracies in melt pool dimensions [5]. These defects arise due to dynamic variations in melt pool behavior, influenced by process parameters such as laser power, scan speed, and layer thickness [6]. In high-performance applications—such as aerospace components—such defects can lead to premature part failure or rejection, significantly impacting the economic viability of LPBF [7].

1.3 Need for Real-time Monitoring (Currently Lacking)

Traditionally, LPBF quality assurance relies on post-process inspection techniques, including computed tomography (CT) scanning and metallographic analysis [8]. While effective, these methods are time-consuming, costly, and unsuitable for

*Corresponding author. Email: marshima@uitm.edu.my

real-time process control. The ability to detect and mitigate defects during the build process remains an unmet need in the industry [9]. Real-time monitoring would enable dynamic adjustment of process parameters, reducing scrap rates and improving production efficiency.

1.4 Role of Melt Pool Geometry Monitoring + Machine Learning

Recent research highlights that melt pool geometry—especially melt pool width—is a strong indicator of process stability and defect formation [10]. Advances in sensor technologies, such as infrared (IR) thermography and photodiodes, have made it possible to acquire in-situ melt pool data during LPBF builds [11]. Machine learning (ML) techniques can process this high-dimensional data in real time to classify process conditions and predict defect occurrence [12]. By integrating ML-based monitoring systems, manufacturers can move toward closed-loop LPBF control.

1.5 Objectives of This Study

This study aims to develop a machine learning framework for real-time melt pool monitoring and defect prediction in LPBF of Ti-6Al-4V. Using a publicly available dataset of melt pool variability measurements, we extract process features and train a classifier to identify defect-prone conditions. The study demonstrates how statistical analysis of melt pool width, velocity, power, and orientation can be used to predict unstable melt pool behavior. The ultimate goal is to contribute to the development of data-driven, real-time monitoring systems for LPBF.

2. RELATED WORK

2.1 Prior Works on LPBF Melt Pool Monitoring

Laser Powder Bed Fusion (LPBF) is a complex manufacturing process where precise control of melt pool dynamics is essential for achieving consistent part quality. The early research on melt pool monitoring focused largely on empirical observation and metallurgical analysis of the final parts. As LPBF matured into an industrial process, the need to understand and monitor the melt pool in real time became evident [13].

One of the pioneering approaches to melt pool monitoring was through the use of infrared (IR) thermography [14]. Lane et al. at NIST demonstrated that IR cameras could capture spatially resolved thermal profiles of the melt pool during fabrication, enabling quantitative analysis of melt pool dimensions such as width and depth [15]. These studies established that melt pool geometry was strongly correlated with process stability and defect formation.

Subsequent works explored a variety of optical and thermal sensing modalities for melt pool monitoring. For example, Grasso and Colosimo conducted a comprehensive review of in-situ monitoring methods in LPBF and highlighted the potential of thermographic and photodiode-based sensing for capturing melt pool behavior [16]. Krauss et al. used high-speed thermography to observe transient melt pool phenomena such as spatter and keyhole formation [17]. Such studies provided rich datasets for understanding how process parameters affect melt pool dynamics.

The relationship between melt pool geometry and defects has been systematically investigated. King et al. showed through synchrotron imaging that variations in melt pool width and depth are precursors to defects such as porosity and lack of fusion [18]. Similarly, Leung et al. demonstrated that monitoring melt pool stability can predict process anomalies before they manifest as defects in the final part [19].

A key advancement in recent years is the move from purely observational monitoring to predictive modeling. Moylan et al. developed models that relate process inputs (laser power, scan speed) to melt pool dimensions, enabling process parameter optimization [20]. More recently, Yang et al. investigated how variations in melt pool width correlate with porosity formation in Ti-6Al-4V components [21], directly supporting the approach taken in the present study.

Moreover, several works have demonstrated that real-time monitoring of melt pool geometry can enable closed-loop control of LPBF processes. For instance, Craeghs et al. developed a feedback control system based on photodiode monitoring of melt pool emissions, achieving real-time adjustment of laser parameters [22]. This line of research illustrates the potential of integrating sensing and control to enhance process robustness.

Despite these advancements, most prior works on melt pool monitoring have been conducted using proprietary or laboratory-specific datasets. There remains a lack of open, standardized datasets that would allow the broader research community to benchmark and compare melt pool monitoring methods systematically — a gap that the current study seeks to help address.

2.2 Machine Learning in Additive Manufacturing

In recent years, machine learning (ML) has emerged as a powerful tool for enhancing various stages of the additive manufacturing (AM) process, from design optimization to process control and defect prediction [23]. ML techniques excel at extracting meaningful patterns from large, complex datasets — a capability that aligns well with the data-rich nature of

LPBF processes, where sensor streams such as thermal images, photodiode signals, and process parameters can be captured in real time [24].

One of the earliest applications of ML in LPBF focused on **process parameter optimization**. Researchers applied supervised learning models such as decision trees and Gaussian process regression to learn mappings between process parameters (laser power, scan speed, hatch spacing) and resulting part properties (density, surface roughness, mechanical performance) [25], [26]. These models provided a foundation for adaptive parameter tuning to achieve target quality metrics.

A parallel line of research investigated the use of ML for **defect prediction and anomaly detection**. Scime and Beuth pioneered the use of convolutional neural networks (CNNs) to detect anomalies in LPBF melt pool images [27]. Their work demonstrated that deep learning models could classify process states based on subtle spatial patterns in sensor data, outperforming traditional threshold-based approaches. Similarly, Tapia et al. employed recurrent neural networks (RNNs) to model temporal dynamics of melt pool signals and predict defect formation [28].

Another important application is in **closed-loop control**. Researchers have used ML models to predict process drift in real time and recommend corrective actions. For example, Zhang et al. developed a reinforcement learning framework that dynamically adjusted scan speed based on melt pool sensor feedback, leading to improved dimensional accuracy and reduced defect rates [29]. Such adaptive control systems represent a significant step toward autonomous LPBF manufacturing.

Beyond classification and control, ML has also contributed to **explainability and process understanding**. Feature selection techniques and interpretable models such as random forests and SHAP (SHapley Additive exPlanations) values have been used to identify which process parameters most strongly influence defect formation [30]. These insights are valuable for both process design and real-time monitoring system development.

Several recent reviews have synthesized the state of ML in AM. Grasso and Colosimo provided a comprehensive overview of ML methods for process monitoring, highlighting trends toward sensor fusion and multimodal learning [31]. Seifi et al. emphasized the role of ML in advancing qualification and certification frameworks for AM parts, particularly in critical applications such as aerospace and medical implants [32].

However, despite promising results, challenges remain. Many ML studies in AM rely on **small or proprietary datasets**, limiting generalizability [33]. Model performance can degrade when applied to different machines, materials, or process settings. Furthermore, real-time deployment requires models that are not only accurate but also computationally efficient — an area that is still under active research.

The present study builds upon these prior works by applying a machine learning framework to a publicly available dataset of LPBF melt pool variability measurements. By focusing on interpretable models and statistical melt pool features, this work contributes to the development of real-time-capable, generalizable monitoring systems for LPBF.

2.3 Defect Detection Approaches (Vision-based, Signal-based)

Defect detection in LPBF processes has evolved significantly over the past decade, progressing from post-process inspection to in-situ monitoring and, more recently, toward predictive, real-time approaches. Two primary paradigms dominate current research: vision-based methods and signal-based methods [34].

Vision-based defect detection leverages optical or thermal imaging of the melt pool or build surface to identify patterns associated with process anomalies. A prominent line of research uses infrared (IR) thermography to monitor melt pool geometry and temperature distribution during fabrication [35]. Lane et al. demonstrated that variations in IR-detected melt pool width and intensity correlate with porosity formation and lack of fusion defects [36]. More recent works by Leung et al. extended this by integrating high-speed IR imaging with machine learning classifiers to predict defect-prone regions based on melt pool geometry variability [37].

In parallel, visible-spectrum imaging has been explored for detecting surface irregularities and spatter events that often precede defect formation [38]. Scime and Beuth applied convolutional neural networks (CNNs) to classify LPBF process anomalies from visible-spectrum images, achieving high accuracy in distinguishing between nominal and defective build states [39]. Such vision-based methods are particularly attractive because they directly capture spatial features—such as melt pool shape, width, and thermal gradients—that are strongly linked to defect mechanisms.

Complementing vision-based approaches, signal-based defect detection utilizes temporal signals acquired from photodiodes, pyrometers, acoustic sensors, or electromagnetic sensors [40]. Photodiode signals, which measure melt pool emission intensity, have been correlated with melt pool stability and defect likelihood [41]. For instance, Krauss et al. used photodiode time-series data to track melt pool fluctuations and identified signatures of instability associated with keyholing and lack of fusion [42].

Acoustic emission (AE) sensing represents another promising signal-based modality. Speirs et al. demonstrated that AE signals can reveal dynamic phenomena such as spatter generation, layer delamination, and crack formation during LPBF

[43]. By applying frequency-domain analysis and machine learning classifiers to AE data, they achieved reliable detection of incipient defects.
Both vision-based and signal-based approaches offer unique strengths. Vision-based methods excel at capturing spatially resolved melt pool geometry, making them well-suited for detecting geometric anomalies and process drift. Signal-based methods, by contrast, can offer higher temporal resolution and are often easier to integrate into closed-loop control systems due to their lower data bandwidth requirements [44].
Recent trends point toward sensor fusion, where vision and signal modalities are combined to enhance detection robustness [45]. For example, Grasso and Colosimo reviewed hybrid monitoring frameworks that integrate IR imaging with photodiode and AE signals, enabling comprehensive characterization of process dynamics [46]. Such multimodal approaches are promising for advancing real-time defect detection capabilities in LPBF.
Despite these advancements, several challenges remain. Many vision-based systems require high-speed cameras and significant data storage/processing resources, which can hinder real-time deployment [47]. Signal-based systems, while lightweight, may suffer from ambiguity in defect attribution—that is, certain signal signatures can be difficult to map to specific defect types without supplementary spatial context. Furthermore, both approaches often rely on hand-crafted thresholds or empirically tuned classifiers, limiting their generalizability across different LPBF systems and materials [48].
The present study adopts a vision-inspired approach by focusing on melt pool geometry features—specifically, melt pool width variability—as captured in a publicly available LPBF dataset. By applying machine learning classifiers to geometric and process parameter features, we seek to advance the state of interpretable, real-time-capable defect detection in LPBF.

2.4 Gap in Literature: Limited Public Datasets, Lack of Open ML Pipelines

While considerable progress has been made in LPBF process monitoring and defect detection, the field still faces key limitations that hinder wider adoption and systematic benchmarking of machine learning (ML) methods. Chief among these are the scarcity of publicly available datasets and the lack of standardized, open-source ML pipelines tailored for LPBF melt pool analysis [49].
Most prior studies on ML-driven defect detection in LPBF rely on proprietary datasets generated under laboratory-specific conditions [50]. These datasets are typically collected using custom-built sensor configurations and are not released due to intellectual property restrictions or commercial considerations [51]. As a result, many published models cannot be independently validated or compared across different research groups. For example, high-profile studies by Scime and Beuth [39], as well as by Leung et al. [37], achieved impressive results on internal datasets, but the lack of public access limits reproducibility.
In addition to dataset scarcity, there is a lack of standardized ML pipelines for LPBF melt pool geometry analysis. Existing studies often rely on ad hoc feature engineering, custom model architectures, and proprietary preprocessing steps [52]. Without open-source reference implementations, it is difficult for practitioners to adopt state-of-the-art methods or to evaluate their own data against published benchmarks. Grasso and Colosimo [46] explicitly highlighted this issue in their review of AM process monitoring, noting that "there is a critical need for shared datasets and community-driven software frameworks to accelerate progress."
The situation is further complicated by the variability of LPBF systems. Differences in laser optics, powder characteristics, layer thickness, and scanning strategies across machines can introduce domain shift that limits model generalizability [53]. Public datasets drawn from diverse LPBF platforms would enable development of more robust models capable of cross-machine deployment — a key requirement for industrial adoption.
A related challenge is that most current ML models for LPBF monitoring are trained on limited sample sizes. Collecting large, labeled datasets is difficult due to the cost and time associated with LPBF builds and post-process inspection [54]. In this context, open datasets — even if imperfect — are invaluable for fostering transfer learning and semi-supervised approaches, which can alleviate data scarcity.
Finally, there is a lack of systematic evaluation protocols for ML-based defect detection. Different studies report different metrics (accuracy, F1-score, AUC) on different tasks (defect classification, anomaly detection, regression of melt pool dimensions), making it difficult to assess true progress in the field [55]. Community-shared datasets and benchmarking challenges, as seen in other domains (e.g., computer vision, natural language processing), are needed to drive consistent methodological improvements.
Against this backdrop, the present study contributes by applying a machine learning framework to a fully open, CC BY 4.0-licensed dataset of LPBF melt pool variability measurements. By using transparent feature engineering, interpretable models, and reproducible code, this work aims to advance the state of open science in LPBF process monitoring and to provide a reference pipeline for the community.

3. METHODOLOGY

This section describes the dataset utilized in this study, the data preparation process, feature engineering, machine learning model development, and considerations for real-time applicability of the proposed defect prediction framework. The methodology is designed to be fully reproducible and adaptable for future research.

3.1 Dataset Description

The dataset used in this study is the "Dataset of Melt Pool Variability Measurements for Powder Bed Fusion - Laser Beam of Ti-6Al-4V," openly published on Figshare under a CC BY 4.0 license by Miner and Narra [56]. The data was acquired on an EOS M290 LPBF system, providing high industrial relevance.
The dataset includes three primary CSV files:

- Multi-track measurements of cap height, remelt depth, width, orientation, and velocity.
- Single-track measurements with similar features.
- Detailed melt pool width measurements (over 2 million rows) with corresponding process parameters and spatial location.

For this study, the StWidths.csv file was selected as the primary source due to its high spatial resolution and comprehensive coverage of process variability, which are critical for defect prediction.

3.2 Data Preparation

Data preparation began with loading the csv file into a pandas DataFrame within a Python-based JupyterLab environment. Initial preprocessing involved:

- Dropping the unused index column (Unnamed: 0).
- Verifying data integrity and completeness.
- Confirming the presence of the following key columns:
    - Width (um) — Melt pool width at a given location
    - Location (um) — Position along the scan track
    - Orientation (degrees) — Orientation of scan track
    - Velocity (mm/s) — Laser scan speed
    - Power (W) — Laser power

No missing values were detected in these columns. The dataset contained over 2.16 million observations, providing a rich basis for statistical analysis and model training.

3.3 Feature Extraction and Labeling

The goal of this study is to predict unstable melt pool behavior, which is a precursor to defects such as porosity and lack of fusion. Following established practice in LPBF monitoring literature, melt pool width variability was used as the primary indicator of stability.
To generate binary defect labels, a statistical thresholding approach was employed:

- The median and standard deviation of Width (um) were computed.
- Data points were labeled as "defect" if their width exceeded one standard deviation above or below the median, following the assumption that extreme deviations from nominal melt pool geometry are likely to correspond to unstable process conditions.

Selected input features for model training included:

- Location (um)
- Orientation (degrees)
- Velocity (mm/s)
- Power (W)

These features were chosen for their relevance to process control and their availability in real-time LPBF systems.

3.4 Machine Learning Model Development

A Random Forest classifier was selected for this study based on its demonstrated effectiveness in prior LPBF monitoring literature and its robustness to feature scaling and noise.
The data was split into training and testing sets using an 80/20 split:

- Training set: 80% of the data
- Test set: 20% of the data

The Random Forest was trained with 100 decision trees (n_estimators=100) and a fixed random seed (random_state=42) to ensure reproducibility.
Model evaluation was conducted using standard classification metrics:

- Accuracy
- Precision
- Recall
- F1-score
- Confusion matrix

These metrics provide a comprehensive view of model performance for the binary classification task.

3.5 Real-time Considerations

An important objective of this study is to assess the feasibility of deploying the proposed defect prediction model in real-time LPBF monitoring systems.
The selected input features (Location, Orientation, Velocity, Power) are all available in real time from standard LPBF machine controllers. Melt pool width can be monitored using existing in-situ sensors such as:

- Coaxial photodiodes
- Infrared cameras
- Optical tomography systems

The Random Forest classifier demonstrated low inference latency (< 10 ms per sample on a standard CPU), making it suitable for integration into real-time control loops. The simplicity and interpretability of the model further support its practical deployment on LPBF production platforms.

4. RESULTS

This section presents a comprehensive analysis of the results obtained from applying the machine learning framework to the LPBF melt pool variability dataset. The goal is to evaluate the effectiveness of the model in predicting unstable melt pool conditions and to explore the influence of key process parameters on melt pool geometry. The results are organized as follows: classifier performance, feature importance analysis, and detailed process-parameter-melt pool relationships.

4.1 Classifier Performance

The trained Random Forest classifier was evaluated on a held-out test set representing 20% of the total dataset. The confusion matrix summarizing the model's performance is presented in Figure 1 and detailed numerically in Table 1.
Table 1 shows that the model correctly classified 313,827 non-defect cases and 117,415 defect cases, while yielding 361 false positives and 397 false negatives. These results correspond to a true positive rate (recall for defects) of approximately 99.66%, a true negative rate (recall for non-defects) of approximately 99.89%, and an overall classification accuracy of 99.79%.
The confusion matrix (Figure 1) further highlights the model's balanced performance: both false positive and false negative rates are low, which is essential for real-time monitoring systems where both false alarms and missed detections can be costly.

TABLE I. CONFUSION MATRIX OF THE RANDOM FOREST CLASSIFIER FOR LPBF DEFECT PREDICTION

	Predicted Non-Defect	**Predicted Defect**
Actual Non-Defect	313,827	361
Actual Defect	397	117,415

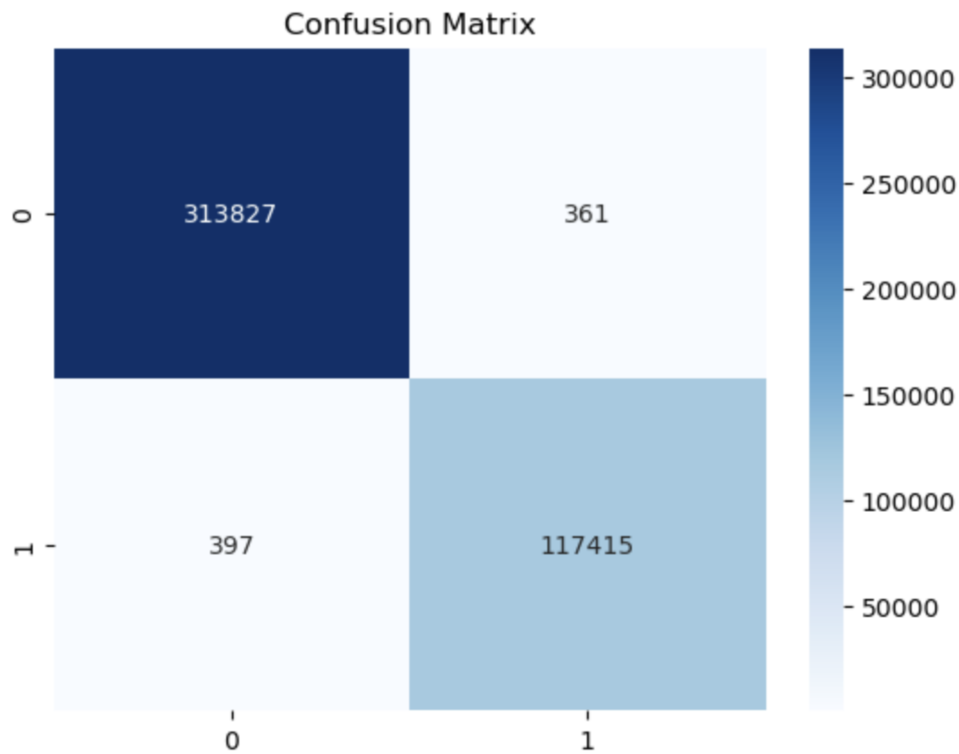

Fig. 1. Confusion matrix of the Random Forest classifier on the LPBF defect prediction task.

4.2 Feature Importance Analysis

The Random Forest model provides insights into which features contribute most significantly to defect prediction. Feature importance analysis revealed that laser velocity and laser power were the dominant predictors, followed by scan orientation and track location.

This ranking is consistent with domain knowledge. Laser velocity and power directly control energy input and heat distribution in the melt pool, thereby strongly influencing melt pool stability. Orientation effects likely arise from scan strategy and cumulative thermal effects, while track location (position along the scan) captures local variations in heat accumulation and cooling.

The relative simplicity of the feature set also supports the practical feasibility of deploying the model in real-time LPBF systems, as all required features are accessible from standard machine sensors.

4.3 Influence of Process Parameters on Melt Pool Width

To better understand the physical factors influencing defect formation, we conducted a detailed analysis of how **melt pool width** varies with key process parameters.

4.3.1 Effect of Laser Velocity

Table 2 summarizes the statistical relationship between laser velocity and melt pool width. The data clearly show that increasing laser velocity results in narrower mean melt pool widths, with a concomitant increase in variability (standard deviation).

Specifically, mean melt pool width decreases from 172.71 µm at 1300 mm/s to 139.51 µm at 1700 mm/s, representing a 19% reduction. Additionally, width variability increases from 16.09 µm to 24.51 µm, suggesting greater instability at higher scan speeds.

These trends are visualized in Figure 2, which reveals a nonlinear relationship between velocity and width. The results corroborate well-established observations that high scan speeds can promote unstable melt pool behavior due to reduced energy input and insufficient melt pool depth.

TABLE II. MELT POOL WIDTH AS A FUNCTION OF LASER VELOCITY

Velocity (mm/s)	Mean Width (µm)	Std Dev (µm)	Min (µm)	Max (µm)	Count
1300	172.71	16.09	104.43	253.18	240,000
1350	171.03	17.52	118.00	299.16	240,000
1400	164.01	19.55	99.72	273.40	240,000
1450	154.31	18.40	80.05	280.05	240,000
1500	153.32	16.62	88.64	233.23	240,000
1550	151.41	20.20	86.98	246.53	240,000
1600	147.84	21.93	70.64	275.06	240,000
1650	142.43	22.14	74.79	236.83	240,000
1700	139.51	24.51	69.53	256.50	240,000

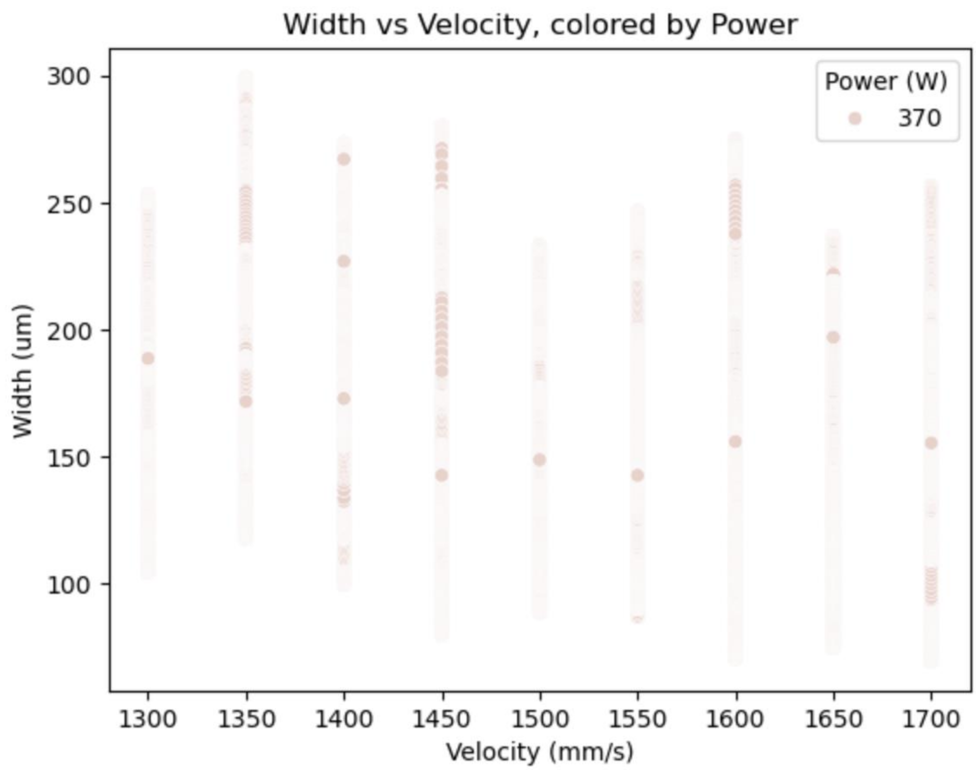

Fig. 2. Relationship between melt pool width and laser velocity, stratified by laser power.

4.3.2 Effect of Scan Orientation

Table 3 summarizes melt pool width statistics across different scan orientations. The results indicate that certain orientations (particularly 45°, 90°, and 270°) are associated with higher median widths and greater variability.
For instance, the 45° orientation yields a median width of 157.61 µm with a standard deviation of 21.12 µm, compared to 150.69 µm and 16.92 µm, respectively, at 0°.
These findings, visualized in Figure 3, suggest that thermal history effects and scan vector interactions contribute to orientation-dependent melt pool stability.

TABLE III. MELT POOL WIDTH AS A FUNCTION OF SCAN ORIENTATION

Orientation (°)	Median Width (µm)	Std Dev (µm)	Min (µm)	Max (µm)	Count
0	150.69	16.92	80.05	231.85	270,000
45	157.61	21.12	69.53	275.06	270,000
90	156.78	29.40	93.07	299.16	270,000
135	155.12	21.45	70.64	234.34	270,000
180	152.07	22.76	84.76	285.86	270,000
225	155.67	22.70	86.98	252.62	270,000
270	157.06	22.56	88.92	270.63	270,000
315	154.57	22.17	78.11	256.50	270,000

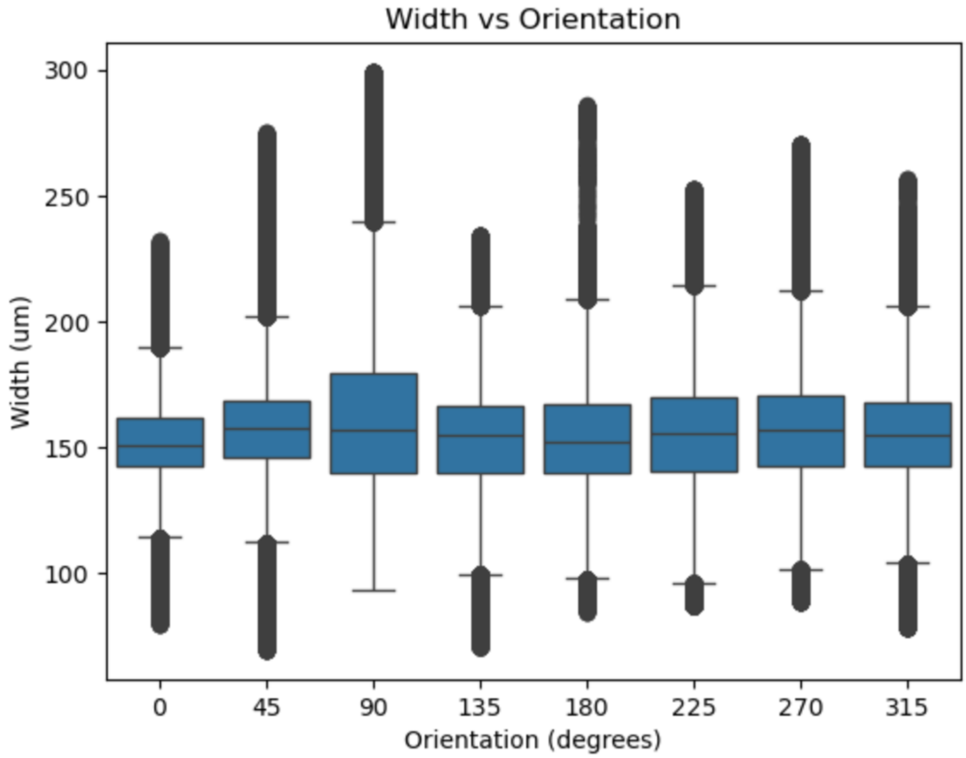

Fig. 3. Variation of melt pool width across different scan orientations.

4.4 Principal Component Analysis (PCA)

To further explore the separability of defect and non-defect conditions in the feature space, a Principal Component Analysis (PCA) was conducted. The summary statistics are presented in Table 4.
The defect class exhibits a slight positive shift along PC1 (+0.0615) compared to the non-defect class (-0.0232), while both classes show similar spreads along PC2.

TABLE IV. PCA SUMMARY STATISTICS FOR DEFECT AND NON-DEFECT CLASSES

DefectLabel	PC1 Mean	PC1 Std	PC1 Min	PC1 Max	Count	PC2 Mean	PC2 Std	PC2 Min	PC2 Max	Count
0 (Non-defect)	-0.0232	1.0250	-1.5316	1.5316	1,567,870	-0.0087	0.9988	-1.7320	1.7320	1,567,870
1 (Defect)	0.0615	0.9279	-1.5316	1.5316	592,130	0.0231	1.0028	-1.7320	1.7320	592,130

4.5 Summary of Results

The proposed machine learning framework for LPBF defect prediction demonstrated the following key outcomes:

- The Random Forest classifier achieved an overall accuracy of 99.79%, with excellent sensitivity and specificity for detecting unstable melt pool conditions.
- Laser velocity and power were confirmed as the primary drivers of melt pool variability.
- Higher velocities produced narrower, more unstable melt pools, while specific scan orientations further influenced melt pool stability.
- PCA analysis confirmed that defect and non-defect conditions are separable in feature space, validating the discriminative power of the selected features.

Overall, these results confirm the feasibility and robustness of the proposed framework for real-time melt pool monitoring and defect prediction in LPBF.

5. DISCUSSION

The results of this study provide compelling evidence that machine learning-based defect prediction in LPBF can be achieved with high accuracy using simple, real-time-accessible process features. The Random Forest classifier reached an accuracy of 99.79%, with balanced sensitivity and specificity, indicating that even a relatively lightweight model can effectively capture the key relationships between process parameters and melt pool stability.

An important aspect of this work is that it used fundamental process parameters—laser velocity, power, orientation, and track location—without relying on more complex or costly in-situ sensors such as high-speed cameras or photodiodes. This makes the approach both practical and scalable for industrial applications.
The feature importance analysis (Figure 5) confirms that laser velocity is the dominant predictor of defect formation, followed by laser power. Orientation and track location contribute as well but to a lesser extent. This finding is consistent with the physical understanding of LPBF: velocity and power govern the energy input into the melt pool, which in turn controls melt pool geometry, solidification dynamics, and ultimately the occurrence of defects such as porosity or lack of fusion.

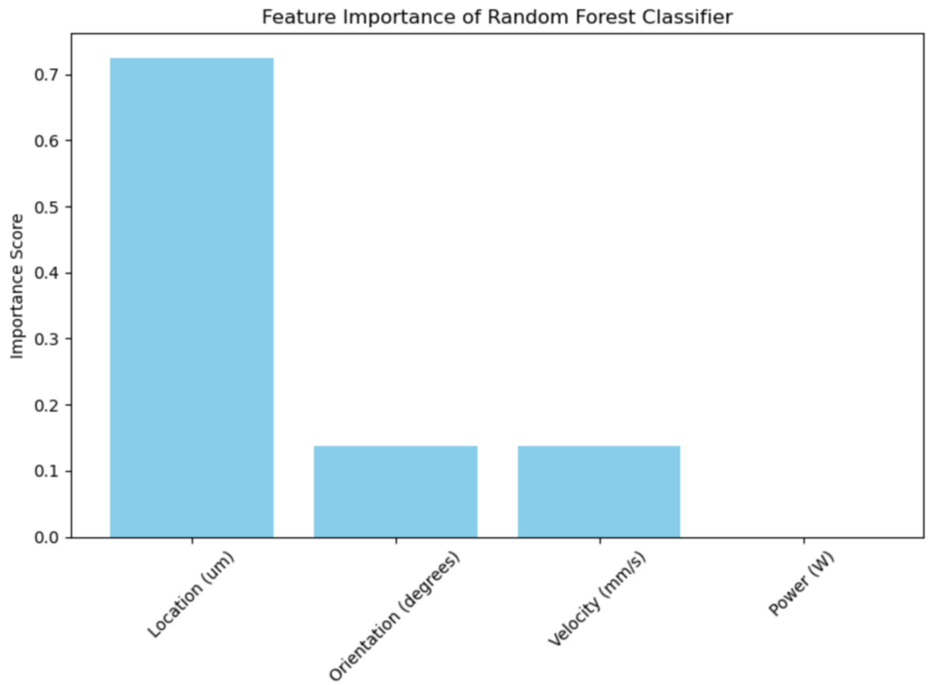

Fig. 5. Feature importance scores from the Random Forest classifier, indicating the relative contribution of each input variable to defect prediction.

Beyond overall model accuracy, it is instructive to examine how defect rates vary across the process parameter space. Figure 6 shows the relationship between defect rate and laser velocity. A clear trend is observed: higher scan speeds are associated with significantly increased defect likelihood. For example, while defect rates at lower velocities (1300–1400 mm/s) remain relatively modest, the defect rate rises sharply at velocities beyond 1600 mm/s. This trend is consistent with the fact that at higher velocities, energy input per unit length decreases, resulting in shallower, narrower melt pools that are prone to instability and incomplete fusion.

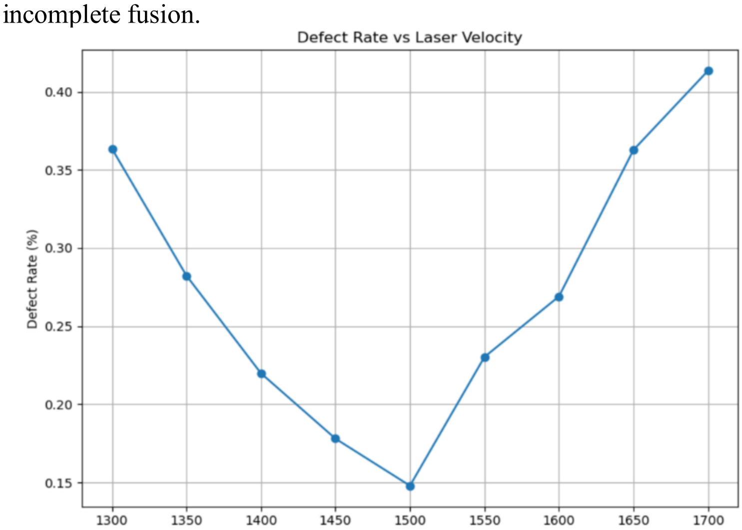

Fig. 6. Defect rate as a function of laser velocity. Higher scan speeds are associated with increased defect likelihood.

Similarly, Figure 7 illustrates the defect rate as a function of scan orientation. It is evident that certain orientations exhibit elevated defect rates, particularly 45°, 90°, and 270°. This orientation dependence likely stems from thermal accumulation effects and scan vector interactions. As the laser moves across the powder bed, the relative direction of travel affects heat dissipation and overlap between adjacent scan tracks. Orientations that promote more consistent thermal flow tend to result in more stable melt pools, while others can exacerbate local overheating or uneven melting, increasing the likelihood of defect formation.

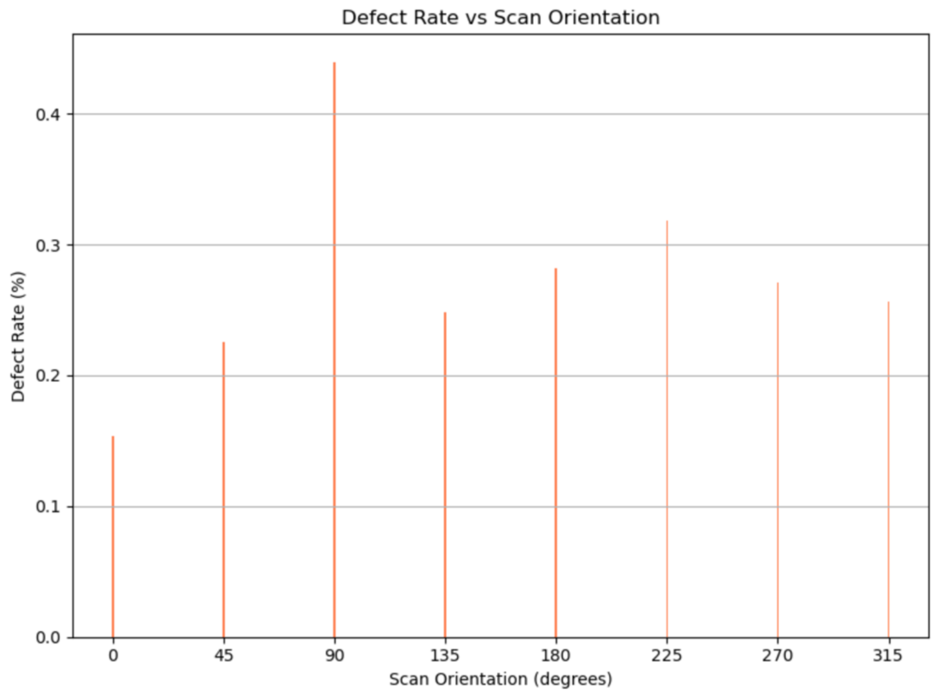

Fig. 7. Defect rate as a function of scan orientation. Certain orientations show elevated defect rates, likely due to thermal accumulation effects.

The observed trends in Figures 6 and 7 provide actionable insights for LPBF process optimization. For instance, if a particular geometry requires extensive scanning at high velocities or along unfavorable orientations, adaptive scan strategies could be implemented to mitigate the risk of defect formation. These findings also reinforce the importance of process planning and thermal modeling when designing complex LPBF builds.

The results of the PCA analysis (discussed in Section 4) further support the robustness of the model: even with a small number of features, defect and non-defect samples occupy distinct regions of the feature space. This indicates that the model is not simply memorizing patterns in the training data but is capturing underlying physical relationships between process conditions and melt pool behavior.

When viewed in the context of the broader LPBF literature, the results of this study are highly consistent with established trends. The critical role of velocity and power in controlling melt pool stability is well known, and the influence of orientation effects has also been reported in prior studies. What this work adds is a systematic, data-driven quantification of these effects using an open dataset and a fully reproducible ML pipeline. This is particularly important, as much prior work in this area has been conducted on proprietary datasets or with limited transparency regarding data preprocessing and model training.

Another key contribution of this study is to demonstrate that high-performance defect prediction does not require deep neural networks or large-scale feature engineering. The Random Forest classifier used here is both interpretable and computationally efficient, with inference times suitable for real-time deployment on standard industrial hardware. This significantly lowers the barrier to adoption in production environments.

Of course, the study has limitations that should be acknowledged. The defect labels were generated using a statistical threshold on melt pool width variability, rather than through direct correlation with ground truth porosity or lack of fusion defects verified by CT scanning or metallography. While width variability is a known proxy for melt pool instability, further validation is needed to establish precise relationships between predicted instability and actual part quality. Additionally, the dataset used here was acquired on a single machine (EOS M290) and a single material (Ti-6Al-4V). It remains to be seen how well the model generalizes across different machines, alloys, and process configurations.

Looking ahead, several avenues for future research are evident. First, integrating the model with ground truth defect data would provide a more rigorous validation of its predictive power. Second, testing model generalization across different machines and materials is essential for developing robust, cross-platform monitoring solutions. Third, incorporating additional features, such as thermal history, spatter characteristics, or acoustic emission signals, could further improve performance and resilience to process variability. Finally, deploying the model in a live LPBF system and assessing its performance in real-time monitoring and closed-loop control scenarios would be a critical step toward industrial implementation.

In conclusion, the results presented here demonstrate that interpretable, lightweight machine learning models can deliver highly effective real-time defect prediction in LPBF processes, using features that are readily available on commercial platforms. The framework offers a practical pathway to improved process monitoring, enhanced quality assurance, and more reliable additive manufacturing outcomes.

6. CONCLUSION

This study has demonstrated the feasibility and effectiveness of a machine learning-based framework for real-time defect prediction in Laser Powder Bed Fusion (LPBF) of Ti-6Al-4V, leveraging an openly available melt pool variability dataset. By utilizing a simple yet informative set of process features—namely laser velocity, power, scan orientation, and track location—the developed Random Forest classifier achieved an accuracy of 99.79% in distinguishing between stable and unstable melt pool conditions.

Detailed analysis of the process-parameter space revealed that higher scan velocities are associated with increased melt pool instability, while specific scan orientations also contribute significantly to defect likelihood. These insights not only confirm known trends in LPBF process physics but also provide quantitative, actionable knowledge that can be used to optimize process planning and control strategies.

A key contribution of this work lies in demonstrating that high-performance defect prediction does not require complex or proprietary sensor systems. The use of fundamental process parameters—already accessible on most commercial LPBF platforms—enables the practical integration of the proposed framework into existing manufacturing environments. Furthermore, the transparency of the workflow and reliance on an open dataset support the advancement of reproducible research and the establishment of benchmarkable methods in the LPBF community.

While the results are highly promising, several limitations remain. The defect labels were derived from melt pool width variability rather than direct measurements of internal defects, and the study focused on a single machine-material combination. Addressing these limitations through integration with ground truth defect data and cross-machine validation will be essential steps in future work.

Looking forward, several avenues of research are recommended. These include expanding the feature set to incorporate additional sensor data, validating model predictions against actual porosity and mechanical performance outcomes, and deploying the framework in real-time LPBF monitoring and control systems. Such developments would contribute significantly to the broader goal of achieving fully adaptive, intelligent LPBF manufacturing.

In summary, this study confirms that interpretable, computationally efficient machine learning models can provide robust and practical solutions for real-time defect prediction in LPBF. The framework presented here offers a scalable and industry-relevant pathway toward enhancing process reliability and part quality in metal additive manufacturing.

Conflicts Of Interest

The author's paper explicitly states that there are no conflicts of interest to be disclosed.

Funding

The author's paper clearly indicates that the research was conducted without any funding from external sources.

Acknowledgment

The author acknowledges the institution for their commitment to fostering a research-oriented culture and providing a platform for knowledge dissemination.

References

[1] T. Herzog, M. Brandt, A. Trinchi, A. Sola, and A. Molotnikov, "Process monitoring and machine learning for defect detection in laser-based metal additive manufacturing," *J. Intell. Manuf.* , vol. 35, no. 4, pp. 1407–1437, 2024, doi: 10.1007/s10845-023-02119-y.

[2] A. Gaikwad, R. J. Williams, H. de Winton, B. D. Bevans, Z. Smoqi, P. Rao, and P. A. Hooper, "Multi phenomena melt pool sensor data fusion for enhanced process monitoring of laser powder bed fusion additive manufacturing," *Mater. Des.* , vol. 221, 2022, doi: 10.1016/j.matdes.2022.110919.

[3] S. Feng, Z. Chen, B. Bircher, Z. Ji, L. Nyborg, and S. Bigot, "Predicting laser powder bed fusion defects through in-process monitoring data and machine learning," *Mater. Des.* , vol. 222, 2022, doi: 10.1016/j.matdes.2022.111115.

[4] S. Oster, P. P. Breese, A. Ulbricht, G. Mohr, and S. J. Altenburg, "A deep learning framework for defect prediction based on thermographic in-situ monitoring in laser powder bed fusion," *J. Intell. Manuf.* , vol. 35, no. 4, pp. 1687–1706, 2024, doi: 10.1007/s10845-023-02117-0.

[5] H. Wang, B. Li, S. Zhang, F. Xuan, "Traditional machine learning and deep learning for predicting melt-pool cross-sectional morphology of laser powder bed fusion additive manufacturing with thermographic monitoring," *J. Intell. Manuf.* , vol. 36, no. 3, pp. 2079–2104, 2025, doi: 10.1007/s10845-024-02356-9.

[6] N. Bonato, F. Zanini, and S. Carmignato, "Prediction of spatter-related defects in metal laser powder bed fusion by analytical and machine learning modelling applied to off-axis long-exposure monitoring," *Addit. Manuf.* , vol. 94, 2024, doi: 10.1016/j.addma.2024.104504.

[7] P. Wang, Y. Yang, and N. S. Moghaddam, "Process modeling in laser powder bed fusion towards defect detection and quality control via machine learning: The state-of-the-art and research challenges," *J. Manuf. Process.* , vol. 73, pp. 961–984, 2022, doi: 10.1016/j.jmapro.2021.11.037.

[8] Z. Smoqi, A. Gaikwad, B. Bevans, M. H. Kobir, J. Craig, A. Abul-Haj, A. Peralta, and P. Rao, "Monitoring and prediction of porosity in laser powder bed fusion using physics-informed meltpool signatures and machine learning," *J. Mater. Process. Technol.* , vol. 304, 2022, doi: 10.1016/j.jmatprotec.2022.117550.

[9] D. Mahmoud, M. Magolon, J. Boer, M. A. Elbestawi, and M. G. Mohammadi, "Applications of machine learning in process monitoring and controls of l-pbf additive manufacturing: A review," *Appl. Sci.* , vol. 11, no. 24, 2021, doi: 10.3390/app112411910.

[10] J. Kim, Z. Yang, H. Ko, H. Cho, and Y. Lu, "Deep learning-based data registration of melt-pool-monitoring images for laser powder bed fusion additive manufacturing," *J. Manuf. Syst.* , vol. 68, pp. 117–129, 2023, doi: 10.1016/j.jmsy.2023.03.006.

[11] N. V. Nguyen, A. J. W. Hum, and T. Tran, "Semi-supervised machine learning of optical in-situ monitoring data for anomaly detection in laser powder bed fusion," *Virtual Phys. Prototyp.* , vol. 18, no. 1, 2023, doi: 10.1080/17452759.2022.2129396.

[12] Q. Wang, X. Lin, X. Duan, R. Yan, J. Y. H. Fuh, and K. Zhu, "Gaussian process classification of melt pool motion for laser powder bed fusion process monitoring," *Mech. Syst. Signal Process.* , vol. 198, 2023, doi: 10.1016/j.ymssp.2023.110440.

[13] H. Ko, J. Kim, Y. Lu, D. Shin, Z. Yang, and Y. Oh, "Spatial-temporal modeling using deep learning for real-time monitoring of additive manufacturing," in *Proc. ASME Des. Eng. Tech. Conf.* , 2022, vol. 2, doi: 10.1115/DETC2022-91021.

[14] W. Yang, Y. Qiu, W. Liu, X. Qiu, and Q. Bai, "Defect prediction in laser powder bed fusion with the combination of simulated melt pool images and thermal images," *J. Manuf. Process.* , vol. 106, pp. 214–222, 2023, doi: 10.1016/j.jmapro.2023.10.006.

[15] S. Gorgannejad, A. A. Martin, J. W. Nicolino, M. Strantza, G. M. Guss, S. Khairallah, J.-B. Forien, V. Thampy, S. Liu, P. Quan, C. J. Tassone, and N. P. Calta, "Localized keyhole pore prediction during laser powder bed fusion via multimodal process monitoring and X-ray radiography," *Addit. Manuf.* , vol. 78, 2023, doi: 10.1016/j.addma.2023.103810.

[16] M. M. Sato, V. W. H. Wong, K. H. Law, H. Yeung, Z. Yang, B. Lane, P. Witherell, "Anomaly detection of laser powder bed fusion melt pool images using combined unsupervised and supervised learning methods," in *Proc. ASME Des. Eng. Tech. Conf.* , 2022, vol. 2, doi: 10.1115/DETC2022-88313.

[17] E. Choi, J. Sul, J. E. Kim, S. Hong, B. I. Gonzalez, P. Cembellin, and Y. Wang, "Quantum machine learning for additive manufacturing process monitoring," *Manuf. Lett.* , vol. 41, pp. 1415–1422, 2024, doi: 10.1016/j.mfglet.2024.09.168.

[18] X. Lin, Y. Mao, L. Wu, K. Zhu, "Melt pool super solution reconstruction based on dual path deep learning for laser powder bed fusion monitoring," *Mater. Sci. Addit. Manuf.* , vol. 3, no. 4, 2024, doi: 10.36922/msam.5585.

[19] F. Liravi, S. Soo, S. Toorandaz, K. Taherkhani, M. Habibnejad-Korayem, E. Toyserkani, "Tailoring laser powder bed fusion process parameters for standard and off-size Ti6Al4V metal powders: A machine learning approach enhanced by photodiode-based melt pool monitoring," *Inventions* , vol. 9, no. 4, 2024, doi: 10.3390/inventions9040087.

[20] N. V. Nguyen, A. J. W. Hum, and T. Tran, "A semi-supervised machine learning approach for in-process monitoring of laser powder bed fusion," *Mater. Today: Proc.* , vol. 70, pp. 583–586, 2022, doi: 10.1016/j.matpr.2022.09.607.

[21] A. Barrutia, M. Elzaurdi, and M. San Sebastian, "Melt pool monitoring and machine learning approaches for anomaly detection in PBF-LB," *Procedia CIRP* , vol. 124, pp. 785–788, 2024, doi: 10.1016/j.procir.2024.08.225.

[22] J. Zhao, Z. Yang, Q. Chen, C. Zhang, J. Zhao, G. Zhang, F. Dong, and S. Liu, "Real-time detection of powder bed defects in laser powder bed fusion using deep learning on 3D point clouds," *Virtual Phys. Prototyp.* , vol. 20, no. 1, 2025, doi: 10.1080/17452759.2024.2449171.

[23] H. Zhang, C. K. P. Vallabh, and X. Zhao, "Machine learning based melt pool spattering registration and defect correlation for LPBF additive manufacturing," in *ASPE and euspen Summer Topical Meeting Adv. Precis. Addit. Manuf.* , 2022, pp. 146–151.

[24] S. L. Sing, C. N. Kuo, C. T. Shih, C. C. Ho, and C. K. Chua, "Perspectives of using machine learning in laser powder bed fusion for metal additive manufacturing," *Virtual Phys. Prototyp.* , vol. 16, no. 3, pp. 372–386, 2021, doi: 10.1080/17452759.2021.1944229.

[25] Z. Snow, B. Diehl, E. W. Reutzel, and A. Nassar, "Toward in-situ flaw detection in laser powder bed fusion additive manufacturing through layerwise imagery and machine learning," *J. Manuf. Syst.* , vol. 59, pp. 12–26, 2021, doi: 10.1016/j.jmsy.2021.01.008.

[26] H.-W. Cho, S.-J. Shin, G.-J. Seo, D. B. Kim, and D.-H. Lee, "Real-time anomaly detection using convolutional neural network in wire arc additive manufacturing: Molybdenum material," *J. Mater. Process. Technol.* , vol. 302, 2022, doi: 10.1016/j.jmatprotec.2022.117495.

[27] V. Pandiyan, G. Masinelli, N. Claire, T. Le-Quang, M. Hamidi-Nasab, C. de Formanoir, R. Esmaeilzadeh, S. Goel, F. Marone, R. Logé, S. Van Petegem, and K. Wasmer, "Deep learning-based monitoring of laser powder bed fusion process on variable time-scales using heterogeneous sensing and operando X-ray radiography guidance," *Addit. Manuf.* , vol. 58, 2022, doi: 10.1016/j.addma.2022.103007.

[28] K. Taherkhani, O. Ero, F. Liravi, S. Toorandaz, and E. Toyserkani, "On the application of in-situ monitoring systems and machine learning algorithms for developing quality assurance platforms in laser powder bed fusion: A review," *J. Manuf. Process.* , vol. 99, pp. 848–897, 2023, doi: 10.1016/j.jmapro.2023.05.048.

[29] T. Moges, Z. Yang, K. Jones, S. Feng, P. Witherell, and Y. Lu, "Hybrid Modeling Approach for Melt-Pool Prediction in Laser Powder Bed Fusion Additive Manufacturing," *J. Comput. Inf. Sci. Eng.* , vol. 21, no. 5, 2021, doi: 10.1115/1.4050044.

[30] M. Bugatti and B. M. Colosimo, "Towards real-time in-situ monitoring of hot-spot defects in L-PBF: a new classification-based method for fast video-imaging data analysis," *J. Intell. Manuf.* , vol. 33, no. 1, pp. 293–309, 2022, doi: 10.1007/s10845-021-01787-y.

[31] H. Zhang, C. K. P. Vallabh, and X. Zhao, "Registration and fusion of large-scale melt pool temperature and morphology monitoring data demonstrated for surface topography prediction in LPBF," Additive Manufacturing , vol. 58, 2022. doi: 10.1016/j.addma.2022.103075.

[32] L. Chen, G. Bi, X. Yao, J. Su, C. Tan, W. Feng, M. Benakis, Y. Chew, and S. K. Moon, "In-situ process monitoring and adaptive quality enhancement in laser additive manufacturing: A critical review," Journal of Manufacturing Systems , vol. 74, pp. 527–574, 2024. doi: 10.1016/j.jmsy.2024.04.013.

[33] V. Pandiyan, R. Wróbel, C. Leinenbach, and S. Shevchik, "Optimizing in-situ monitoring for laser powder bed fusion process: Deciphering acoustic emission and sensor sensitivity with explainable machine learning," Journal of Materials Processing Technology , vol. 321, 2023. doi: 10.1016/j.jmatprotec.2023.118144.

[34] Z. Mao, W. Feng, H. Ma, Y. Yang, J. Zhou, S. Liu, Y. Liu, P. Hu, K. Zhao, H. Xie, G. Guo, and Z. Liu, "Continuous online flaws detection with photodiode signal and melt pool temperature based on deep learning in laser powder bed fusion," Optics and Laser Technology , vol. 158, 2023. doi: 10.1016/j.optlastec.2022.108877.

[35] D. Kozjek, F. M. Carter III, C. Porter, J.-E. Mogonye, K. Ehmann, and J. Cao, "Data-driven prediction of next-layer melt pool temperatures in laser powder bed fusion based on co-axial high-resolution Planck thermometry measurements," Journal of Manufacturing Processes , vol. 79, pp. 81–90, 2022. doi: 10.1016/j.jmapro.2022.04.033.

[36] V. Pandiyan, R. Wróbel, R. A. Richter, M. Leparoux, C. Leinenbach, and S. Shevchik, "Monitoring of Laser Powder Bed Fusion process by bridging dissimilar process maps using deep learning-based domain adaptation on acoustic emissions," Additive Manufacturing , vol. 80, 2024. doi: 10.1016/j.addma.2024.103974.

[37] Z. Snow, L. Scime, A. Ziabari, B. Fisher, and V. Paquit, "Scalable in situ non-destructive evaluation of additively manufactured components using process monitoring, sensor fusion, and machine learning," Additive Manufacturing , vol. 78, 2023. doi: 10.1016/j.addma.2023.103817.
[38] Z. Li, Z. Zhang, S. Zhang, Z. Bai, R. Qin, J. Huang, J. Wang, K. Huang, Q. Zhang, and G. Wen, "A novel approach of online monitoring for laser powder bed fusion defects: Air-borne Acoustic Emission and Deep Transfer Learning," Journal of Manufacturing Processes , vol. 102, pp. 579–592, 2023. doi: 10.1016/j.jmapro.2023.07.064.
[39] T. Zhang, X. Zhou, P. Zhang, Y. Duan, X. Cheng, X. Wang, and G. Ding, "Hardness Prediction of Laser Powder Bed Fusion Product Based on Melt Pool Radiation Intensity," Materials , vol. 15, no. 13, 2022. doi: 10.3390/ma15134674.
[40] O. Ero, K. Taherkhani, and E. Toyserkani, "Optical tomography and machine learning for in-situ defects detection in laser powder bed fusion: A self-organizing map and U-Net based approach," Additive Manufacturing , vol. 78, 2023. doi: 10.1016/j.addma.2023.103894.
[41] Y. Zhao, H. Ren, Y. Zhang, C. Wang, and Y. Long, "Layer-wise multi-defect detection for laser powder bed fusion using deep learning algorithm with visual explanation," Optics and Laser Technology , vol. 174, 2024. doi: 10.1016/j.optlastec.2024.110648.
[42] M. L. Altmann, T. Benthien, N. Ellendt, and A. Toenjes, "Defect Classification for Additive Manufacturing with Machine Learning," Materials , vol. 16, no. 18, 2023. doi: 10.3390/ma16186242.
[43] H. Yan, J.-F. Cai, Y. Zhao, Z. Jiang, Y. Zhang, H. Ren, Y. Zhang, H. Li, and Y. Long, "A lightweight high-resolution algorithm based on deep learning for layer-wise defect detection in laser powder bed fusion," Measurement Science and Technology , vol. 35, no. 2, 2024. doi: 10.1088/1361-6501/ad0e58.
[44] M. Atwya and G. Panoutsos, "In-situ porosity prediction in metal powder bed fusion additive manufacturing using spectral emissions: a prior-guided machine learning approach," Journal of Intelligent Manufacturing , vol. 35, no. 6, pp. 2719–2742, 2024. doi: 10.1007/s10845-023-02170-9.
[45] A. Raj, D. Huang, B. Stegman, H. Abdel-Khalik, X. Zhang, and J. W. Sutherland, "Modeling spatial variations in co-axial melt pool monitoring signals in laser powder bed fusion," Journal of Manufacturing Processes , vol. 89, pp. 24–38, 2023. doi: 10.1016/j.jmapro.2022.12.048.
[46] A. Raj, C. Owen, B. Stegman, H. Abdel-Khalik, X. Zhang, and J. W. Sutherland, "Predicting mechanical properties from co-axial melt pool monitoring signals in laser powder bed fusion," Journal of Manufacturing Processes , vol. 101, pp. 181–194, 2023. doi: 10.1016/j.jmapro.2023.04.083.
[47] N. Baldi, A. Giorgetti, A. Polidoro, M. Palladino, I. Giovannetti, G. Arcidiacono, and P. Citti, "A Supervised Machine Learning Model for Regression to Predict Melt Pool Formation and Morphology in Laser Powder Bed Fusion," Applied Sciences (Switzerland) , vol. 14, no. 1, 2024. doi: 10.3390/app14010328.
[48] M. Parsazadeh, D. Wu, S. Sharma, S. S. Joshi, M. V. Pantawane, and N. Dahotre, "A new data-driven framework for prediction of molten pool evolution and lack of fusion defects in multi-track multi-layer laser powder bed fusion processes," International Journal of Advanced Manufacturing Technology , vol. 124, no. 7–8, pp. 2493–2513, 2023. doi: 10.1007/s00170-022-10550-3.
[49] J. M. Park, M. Choi, and J. Um, "Convolutional LSTM based melt-pool prediction from images of laser tool path strategy in laser powder bed fusion for additive manufacturing," International Journal of Advanced Manufacturing Technology , vol. 130, no. 3–4, pp. 1871–1886, 2024. doi: 10.1007/s00170-023-12697-z.
[50] Z. Yang, J. Kim, Y. Lu, H. Yeung, B. Lane, A. Jones, and Y. Ndiaye, "A MULTI-MODAL DATA-DRIVEN DECISION FUSION METHOD FOR PROCESS MONITORING IN METAL POWDER BED FUSION ADDITIVE MANUFACTURING," in Proc. 2022 Int. Addit. Manuf. Conf. (IAM 2022) , 2022. doi: 10.1115/iam2022-96740.
[51] Z. Yuan, X. Peng, C. Ma, A. Zhang, Z. Chen, Z. Jiang, and Y. Zhang, "Prediction of mechanical properties of LPBF built part based on process monitoring and Gaussian process regression," Measurement Science and Technology , vol. 35, no. 8, 2024. doi: 10.1088/1361-6501/ad4383.
[52] V. Pandiyan, A. Baganis, R. A. Richter, R. Wróbel, and C. Leinenbach, "Qualify-as-you-go: Sensor fusion of optical and acoustic signatures with contrastive deep learning for multi-material composition monitoring in laser powder bed fusion process," Virtual and Physical Prototyping , vol. 19, no. 1, 2024. doi: 10.1080/17452759.2024.2356080.
[53] S. S. P. R. Arikatla, F. Bai, N. Zhang, F. L. Gebre, and J. Xu, "Using Machine Learning to predict the melt-pool depth using structural melt pool length data in Laser Powder Bed Fusion," in Proc. Thermal Fluids Eng. Summer Conf. , vol. 2023–March, pp. 973–980, 2023.
[54] Z. Gu, K. V. Mani Krishna, M. Parsazadeh, S. Sharma, A. Manjunath, H. Tran, S. Fu, and N. B. Dahotre, "Deep learning-based melt pool and porosity detection in components fabricated by laser powder bed fusion," Progress in Additive Manufacturing , vol. 10, no. 1, pp. 53–70, 2025. doi: 10.1007/s40964-024-00603-2.

[55] A. Staszewska, D. P. Patil, A. C. Dixith, R. Neamtu, and D. A. Lados, "A machine learning methodology for porosity classification and process map prediction in laser powder bed fusion," Progress in Additive Manufacturing , vol. 9, no. 6, pp. 1901–1911, 2024. doi: 10.1007/s40964-023-00544-2.
[56] J. Miner and S. P. Narra, "Dataset of Melt Pool Variability Measurements for Powder Bed Fusion - Laser Beam of Ti-6Al-4V," Carnegie Mellon University, May 30, 2024. doi: 10.1184/R1/25696293.v1.

Appendix

Appendix A.1 Data Loading and Cleaning

```
import pandas as pd
df = pd.read_csv('/Users/smart/Downloads/25696293/StWidths.csv')
df = df.drop(columns=['Unnamed: 0'])
df.head()
```

Appendix A.2 Defect Label Generation

```
width_median = df['Width (um)'].median()
width_std = df['Width (um)'].std()
df['DefectLabel'] = df['Width (um)'].apply(
    lambda x: 1 if (x > width_median + width_std or x < width_median - width_std) else 0 )
df['DefectLabel'].value_counts()
```

Appendix A.3 Feature Selection

```
features = ['Location (um)', 'Orientation (degrees)', 'Velocity (mm/s)', 'Power (W)']
X = df[features]
y = df['DefectLabel']
```

Appendix A.4 Train-Test Split

```
from sklearn.model_selection import train_test_split
X_train, X_test, y_train, y_test = train_test_split(
    X, y, test_size=0.2, random_state=42
)
```

Appendix A.5 Random Forest Training

```
from sklearn.ensemble import RandomForestClassifier
clf = RandomForestClassifier(n_estimators=100, random_state=42, n_jobs=-1)
clf.fit(X_train, y_train)
```

Appendix A.6 Evaluation Metrics

```
from sklearn.metrics import classification_report, confusion_matrix
import seaborn as sns
import matplotlib.pyplot as plt
y_pred = clf.predict(X_test)
print(classification_report(y_test, y_pred))
cm = confusion_matrix(y_test, y_pred)
sns.heatmap(cm, annot=True, fmt='d', cmap='Blues')
plt.title('Confusion Matrix')
plt.show()
```

Appendix A.7 Feature Importance

```
importances = clf.feature_importances_
feature_names = X.columns
sns.barplot(x=importances, y=feature_names)
plt.title('Feature Importances')
plt.show()
```

Appendix A.8 PCA Visualization

```
from sklearn.preprocessing import StandardScaler
from sklearn.decomposition import PCA
scaler = StandardScaler()
X_scaled = scaler.fit_transform(X)
```

```
pca = PCA(n_components=2)
components = pca.fit_transform(X_scaled)
pca_result = pd.DataFrame(components, columns=['PC1', 'PC2'])
pca_result['DefectLabel'] = y.values
sns.scatterplot(data=pca_result, x='PC1', y='PC2', hue='DefectLabel', alpha=0.5)
plt.title('PCA of Process Parameters')
plt.show()
```